The 2010 IEEE/RSJ International Conference on
Intelligent Robots and Systems
October 18-22, 2010, Taipei, Taiwan

Circle Fitting Based Position Measurement System Using Laser Range Finder in Construction Fields

Hajime Tamura, *Student Member, IEEE*, Takeshi Sasaki, *Member, IEEE*,
Hideki Hashimoto, *Fellow, IEEE*, and Fumihiro Inoue

***Abstract*— In this paper, an accurate long-distance position measurement system using laser range finders (LRFs), which can be used for surveys in construction fields is proposed. Since the LRF is a sensor which can measure distance to surfaces of objects by radiating laser beams from itself and receiving the reflected ones, data obtained from the LRF are nothing more than the contours of objects. For this reason, we adopted cylindrical shaped objects since the contour, a circular arc, is invariant against rotation. Therefore, this research aims to fit circles to the arc-shaped contours of the cylindrical objects and estimate their accurate center positions by applying the least square method and maximum likelihood estimation. If we know the radius of the cylindrical object in advance, the aforementioned two methods become non-linear problems. For this reason, we applied the Newton-Raphson method to solve these non-linear equations. We improve the angular resolution of the LRF by using a pan unit, and reveal that the maximum likelihood estimation can give us the most accurate center position. Additionally, we implemented proposed position measurement system in an actual construction field.**

I. Introduction

Real-time position measurement for specified objects such as humans or mobile robots by using LRFs is an important task in the research area of so called Intelligent Space (iSpace) which is a space with distributed sensors and actuators [1] [2]. Position measurement using LRFs can also be applied to surveying tasks in construction fields.

In most construction fields, we often need to put a mark on a certain position and, in most cases, these surveying tasks are performed by a Total Station [3]. Although this device can survey with high accuracy, it has several disadvantages: *1. it is impossible to track multiple objects at once, 2. it is impossible to track in real-time, and 3. it is too expensive to purchase or even to rent*. To overcome such problems, we propose a position measurement system using LRFs as shown in Fig. 1.

In the proposed system, a worker moves in the construction field, carrying a reference bar and it is detected by multiple LRFs set at a higher position than human height. This real-time position measurement system is low-cost according to the price of the LRF, and can measure multiple positions at once when multiple reference bars are used, which leads to working hour efficiency. Also by carrying a mobile display device (e.g. a PDA or laptop), and displaying the positions of the reference bars on a map, the workers can easily gain information on where they are and where objective points are in the construction field through a wireless network.

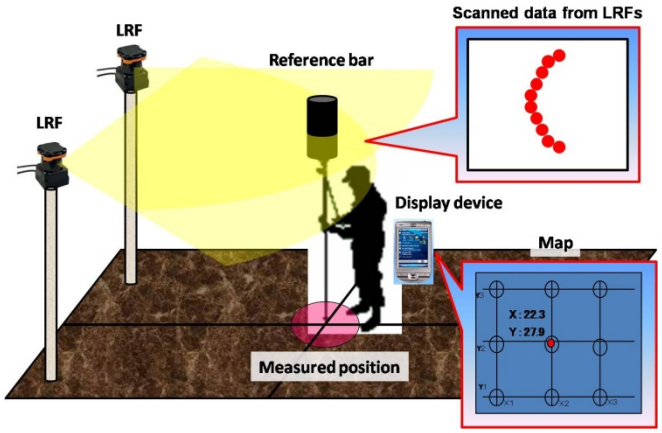

Fig. 1 Proposed position measurement system using LRFs.

However, since data from the LRFs are nothing more than the contour of the reference bar, we need to estimate its center position based on its contour. For this reason, we adopted cylindrical shaped reference bars, which will make the contour of the reference bar a circular arc irrespective of the direction from which it is scanned. Therefore, this research aims to fit circles to the arc-shaped contours of the cylindrical reference bars and estimate their accurate center positions.

Fitting a circle or an ellipse to the observed data points from sensors is a hot topic in the research area of mobile robot navigation and computer vision. In the former case, natural products with geometric features such as a circle or an ellipse are widely used as landmarks of environments. Landmarks such as tree trunks or power poles are usually scanned by LRFs mounted on a mobile robot in order to correct its self-localization [4], [5]. In the latter case, since circular or spherical objects in 3D space are generally projected to an ellipse when they are captured by a camera, an ellipse fitting in the 2D image plane is useful to analyze 3D positions of the objects. This is one of the basic processing techniques in pervasive applications including robot vision [6]-[9]. These circle or ellipse fittings are collectively called *geometric fitting* and there are three main methods to solve this: the Hough transformation [10], the least square method (LSM) [11], and the maximum likelihood estimation (MLE) [12]. However, the Hough transformation is known to require considerable computational resources and consume a huge amount of memory since accurate geometric fitting needs high-density cells. Therefore, we adopted the other two

H. Tamura, T. Sasaki, and H. Hashimoto are with the Institute of Industrial Science, the University of Tokyo, Meguro-ku, Tokyo, 153-8505, Japan (phone: +81-3-5452-6258; fax: +81-3-5452-6259; e-mail: {tamura, sasaki}@ hlab.iis.u-tokyo.ac.jp, hashimoto@iis.u-tokyo.ac.jp).

F. Inoue is with the Technical Research Institute, Obayashi Corporation, Kiyose-shi, Tokyo, 204-8558, Japan (phone:+81-42-495-1275; fax: +81-42-495-0940; e-mail: inoue.fumihiro@obayashi.co.jp)

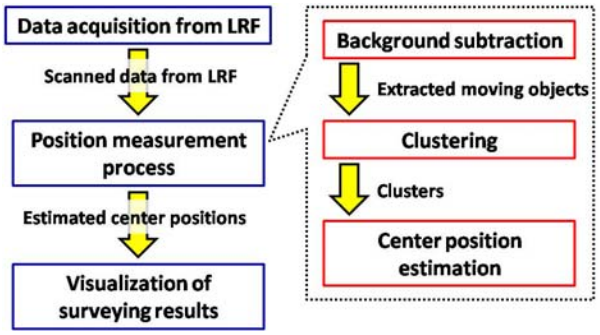

Fig. 2 A system configuration of the proposed position measurement system.

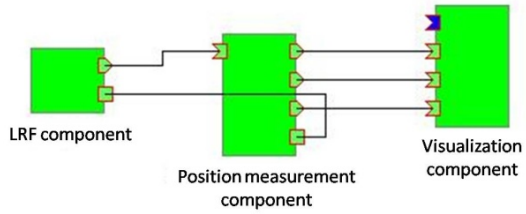

Fig. 3 A system configuration by combining RT-components.

methods; the LSM and the MLE to fit a circle equation to observed data points from an LRF.

Additionally, since we already knew the radius of the reference bar, the parameters we needed to search for were the center position only. Therefore, there is a possibility that we can estimate the center position more accurately when we specify the radius in advance. In the aforementioned two research areas, there are no works in which the LSM and the MLE are applied with known radius.

Moreover, proposed position measurement system should have a capability to flexibly expand measurable area according to the size of the construction field and to easily construct a network among all LRFs and display devices. So we implemented the proposed position measurement system by using RT-Middleware [13] which is being developed by the National Institute of Advanced Industrial Science and Technology (AIST) in Japan. RT-Middleware is a software platform which can be easily used to construct a complex system like a robot by combining each modularized functional component called RT-component. It provides an execution environment to construct whole system by connecting all RT-components distributed on the network transparently, exceeding a wall of different OSs and programming languages. This transparent connection is done by CORBA (Common Object Request Broker Architecture), a distributed object middleware.

In this paper, as a basic research, we focus on making use of single LRF, and aim at establishing an algorithm to fit circles to the arc-shaped contours of the cylindrical reference bars and estimate their accurate center positions and also establishing the most basic position measurement system using RT-Middleware.

II. System Configuration

The proposed position measurement system basically consists of three modules as shown in a left side of the Fig. 2: data acquisition from an LRF, position measurement process, and visualization of surveying results. We established each RT-component so that it will correspond to each module's function. By connecting each RT-component and activating them as shown in Fig. 3, the whole system will be configured. Also we describe I/O information of each RT-component in Table I. Details of each RT-component are described below.

TABLE I
I/O information of each RT-component

Component	Input	Output
LRF	—	Distance Reflected intensity Sensor information
Position measurement	Distance Reflected intensity Sensor information	Center position Contour data Background data
Visualization	Center position Contour data Background data	—

TABLE II
Specification of UTM-30LX

Model Number	UTM-30LX
Light source	Laser diode λ=870[nm]
Measurable area	0.1[m]-30[m], 270[deg]
Measurement accuracy	0.1[m]-10[m] :±30[mm] 10[m]-30[m] :±50[mm]
Angular resolution	0.25[deg]

A. Data acquisition from an LRF

An RT-component in charge of data acquisition from an LRF outputs both a distance to an object's surface and the reflected intensity of each scanning step. We used the UTM-30LX, LRF in our system, from Hokuyo Automatic Co., Ltd. A specification of the UTM-30LX is shown in Table II [14].

B. Position measurement process

An RT-component in charge of the position measurement process receives the aforementioned data from the LRF component and outputs the center position, contour data of the object, and background data. This RT-component consists of three steps as shown on the right side of Fig. 2: background subtraction, clustering of foreground objects, and estimation of the center position of each foreground object. Background subtraction is a step to distinguish moving objects (foreground) from static objects (background). After clustering moving objects by using a nearest neighbor method, we fit circles to the arc-shaped contours and estimate their accurate center positions by using the aforementioned two methods; the LSM and the MLE. Details of these two methods are described below.

1) Least square method (LSM): Generally, the equation of a circle in 2D plane can be expressed as

$$x^2 + y^2 - 2ax - 2by + a^2 + b^2 - r^2 = 0\,, \qquad (1)$$

, where a and b are the center position and r is the radius of the circle. The LSM for a circle is a method for estimating parameters a, b, and r which will minimize the square sum of the error J_{LS} [11] expressed as

$$J_{LS}=\sum_{\alpha=1}^{N}\left(x_\alpha^{\,2}+y_\alpha^{\,2}-2ax_\alpha-2by_\alpha+a^2+b^2-r^2\right)^2, \qquad (2)$$

where $(x_\alpha, y_\alpha), \alpha = 1,...,N$ are the observed data points belonging to the contour of the reference bar.

2) Maximum likelihood estimation (MLE): The MLE for a circle is a method for deciding the parameters *a*, *b*, and *r* so that the observed data can most easily be obtained from the assumed noise model [12]. In other words, the MLE is a method for deciding the parameters *a*, *b*, and *r* which will maximize the likelihood of each data point $(x_\alpha, y_\alpha), \alpha = 1,...,N$. In this paper, we assumed that each data point obtained from the LRF had an independent error described by a Gaussian distribution with mean 0 and standard deviation σ. Then, the likelihood of each data point $(x_\alpha, y_\alpha), \alpha = 1,...,N$ can be expressed as

$$\begin{aligned} &p(x_1,...,x_N,y_1,...,y_N)\\ &=\prod_{\alpha=1}^{N}\frac{exp\left[-(x_\alpha-\bar{x}_\alpha)^2/2\sigma^2\right]}{\sqrt{2\pi\sigma^2}}\times\frac{exp\left[-(y_\alpha-\bar{y}_\alpha)^2/2\sigma^2\right]}{\sqrt{2\pi\sigma^2}}\\ &=\frac{exp\left[-\sum_{\alpha=1}^{N}\left[(x_\alpha-\bar{x}_\alpha)^2+(y_\alpha-\bar{y}_\alpha)^2\right]/2\sigma^2\right]}{\sqrt{(2\pi\sigma^2)^{2N}}} \end{aligned}, \qquad (3)$$

where $(\bar{x}_\alpha, \bar{y}_\alpha)$ is the true position of (x_α, y_α). To maximize this likelihood $p(x_1,...,x_N,y_1,...,y_N)$, we minimize $-\log[p(x_1,...,x_N,y_1,...,y_N)]$. After taking a logarithm of both sides of (3) and removing a constant term which doesn't contribute to minimization, the MLE is equal to minimize following equation J_{ML} defined in (4).

$$J_{ML}=\sum_{\alpha=1}^{N}\frac{\left[(x_\alpha-\bar{x}_\alpha)^2+(y_\alpha-\bar{y}_\alpha)^2\right]}{\sigma^2}. \qquad (4)$$

However, here we have to fulfill (1) as a constraint. After removing the restraint condition by using Lagrange's method of undetermined multipliers, finally the MLE for a circle is equal to estimate parameters *a*, *b*, and *r* which will minimize J_{ML} expressed as

$$J_{ML}=\sum_{\alpha=1}^{N}\frac{\left(x_\alpha^{\,2}+y_\alpha^{\,2}-2ax_\alpha-2by_\alpha+a^2+b^2-r^2\right)^2}{x_\alpha^{\,2}+y_\alpha^{\,2}-2ax_\alpha-2by_\alpha+a^2+b^2}. \qquad (5)$$

Since the radius of the reference bar is given in advance, parameters which should be demanded become only *a* and *b*. However, in this case, both the LSM and the MLE become non-linear problems. In order to solve these non-linear equations, we applied the Newton-Raphson method since it is known to have a faster convergence than other Gradient method, Conjugate gradient method or Levenberg-Marquardt method if its initial value is close to the true value of *a* and *b*.

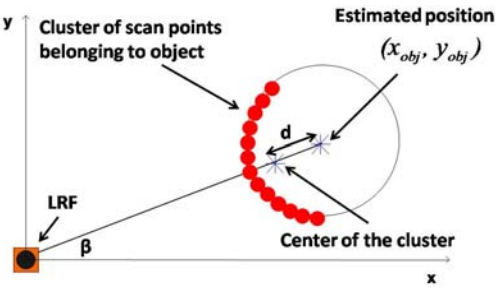

Fig. 4 A principle of the constant distance method (CDM).

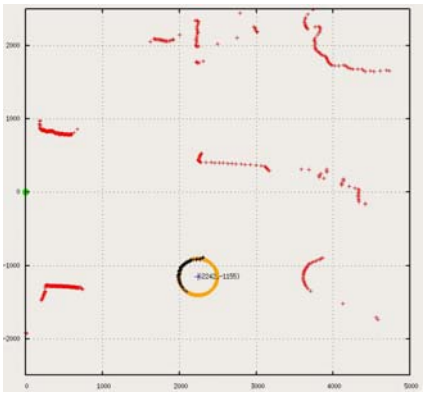
Fig. 5 An example of measuring the center position of the cylindrical reference bar. The unit of x and y are in [mm], and an LRF is set at the origin indicated by a green point. Red points represent background data, black points represent the contour of the reference bar, orange points represent a superimposed circle, and blue point represents measured center position.

Although we can apply the estimated center positions of the LSM and the MLE with unknown radius to the initial value of the Newton-Raphson method, these estimated positions are known to separate from the true value of *a* and *b* when the noise of the arc-shaped contour becomes pronounced [15]. For this reason, we applied the estimated center positions of the *Constant Distance Method* (CDM) [16] as the initial value of the Newton-Raphson method. This method defines a position advanced by a constant *d* from the cluster's center as a center position of the object (x_{obj}, y_{obj}) as shown in Fig. 4. The CDM can estimate an object's center position with a certain amount of accuracy irrespective of its shape.

C. *Visualization of surveying results*

In order to visualize surveying results and make it easier for workers to understand, we used a visualization component which was developed by using a graphical tool *gnuplot* [17]. This component receives data from position measurement process component and displays the surveying results as shown in Fig. 5.

III. EXPERIMENT

A. *Experimental setup*

In order to evaluate estimate errors of the proposed non-linear LSM and non-linear MLE with known radius, and also for comparison the CDM used as the initial value of these two non-linear methods, we performed outdoor experiments by using a single LRF (the aforementioned UTM-30LX) and a cylindrical reference bar whose radius was set to be 250 mm.

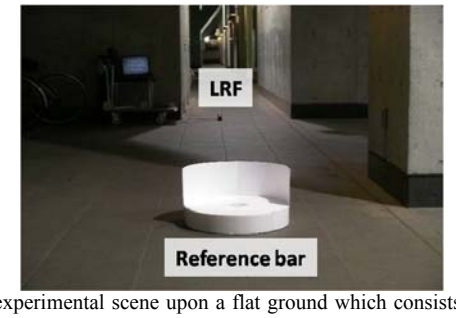

Fig. 6 An experimental scene upon a flat ground which consists of squared tiles. We put the cylindrical reference bar along a line in front of the LRF from 6[m] to 30[m] by 2[m] intervals. Intersections of each tile are used as a reference of a global coordinate.

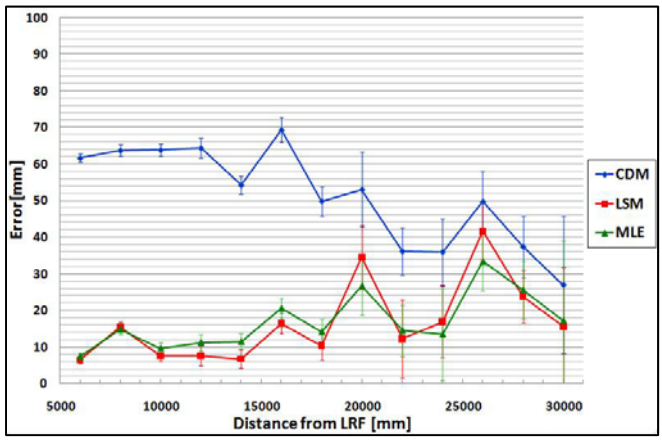

Fig. 7 A comparison of estimate errors of three methods. Blue, red, and green points represent estimate error of the CDM, the LSM, and the MLE in turn.

Since scanned data from the LRF significantly change depending on the material of the surface, we attached a white paper, which has high reflectance in an infrared region, to the cylinder's surface.

This time, we performed experiments upon a flat ground as shown in Fig. 6 in order to avoid unexpected errors derived from slight swings of human hands. Also this flat ground consists of squared tiles and we regarded each intersection as a reference of a distance from the LRF. We put the cylindrical reference bar along a line in front of the LRF from 6 m to 30 m by 2 m intervals. The reason why we started measurements from 6[m] is that the LRF, UTM-30LX was reported to output shorter distance than an original value in an adjacent area to the LRF.

We evaluated estimate errors of the aforementioned three methods: the CDM in which a constant d was set to be 250 mm, the non-linear LSM, and the non-linear MLE with known radius. Estimate error E is defined as

$$E=\sqrt{(X_W-a)^2+(Y_W-b)^2}\,, \tag{6}$$

where (a,b) is the estimated center position of the cylindrical reference bar and (X_W,Y_W) is a position where we put the cylindrical reference bar.

B. Consideration of each method's estimate error

Estimate errors of the aforementioned three methods are shown in Fig. 7. The horizontal axis represents the distance from the LRF and the vertical axis represents the estimate error of each method. Moreover, an error bar shows the standard deviation of the estimate error at each distance. From Fig. 7, although we revealed that the non-linear LSM and the non-linear MLE with known radius which are the novel approaches to estimate the center position of the circle gave fewer errors than that of the CDM, we can say that depending on the increase of distance from the LRF, the error of the CDM tends to decrease and each error of the LSM and the MLE tends to increase. An explanation to these experimental results is described below based on observed data at different distances from the LRF as shown in Fig. 8.

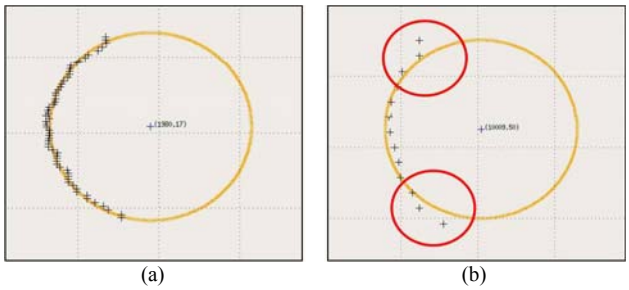

(a) (b)

Fig. 8 The cylinder's contour scanned (a) at a near distance, (b) at a far distance. We can see that noise around the circle's edge became pronounced and the contour became no longer an arc-shaped at a far distance indicated by two red circles.

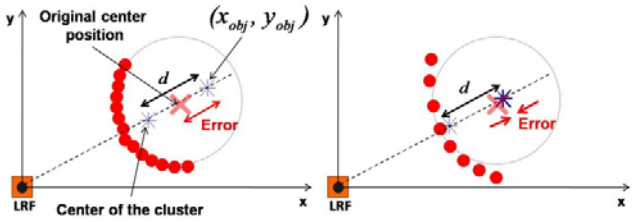

(a) (b)

Fig. 9 Estimate errors of the CDM (a) at a near distance, (b) at a far distance. Depending on the increase of distance, the error in a depth direction decreases.

From Fig. 8, we can see that although the contour of the cylindrical reference bar remained arc-shaped at a near distance, noise around the circle's edge became pronounced and the contour became no longer arc-shaped at a far distance. This is because a reflection from the circle's edge becomes only a slightly diffused element in a far distance, which makes both the S/N ratio and the shape of the contour worse. Finally, it became a linear shape at more than 20 m. Additionally, we can see that data points belonging to the contour decreased at a far distance. This is because an angular resolution of the LRF set as 0.25 deg, which makes a density of a laser beam sparse at a far distance from the LRF. These two phenomena are considered to be the reason why each error of the LSM and the MLE tends to increase at a far distance.

Also with respect to the CDM, the tendency with which its error tends to decrease at a far distance is considered to be due to the aforementioned collapse of the contour's shape and also a constant d set to be the same value as the radius of the cylinder, 250 mm as shown in Fig. 9. At a near distance, since the contour is the arc-shaped, the center of the cluster is placed further away from the contour, which makes the

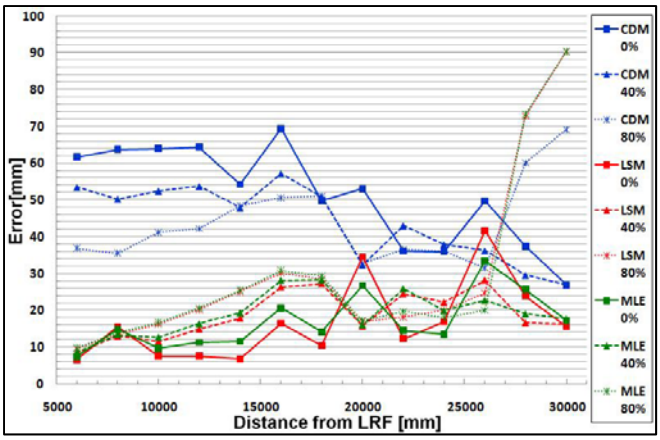

Fig. 10 Estimate errors of the three methods with a reflected beam intensity filter whose filtering threshold was set to be 0%, 40%, and 80% represent by the continuous, the broken, and the dotted line in turn. The sharp rises at more than 28[m] are considered to be due to an extreme lack of the number of data points. The error bars are omitted to avoid confusing.

estimated position advanced by 250 mm from it pass over the true center position and the estimate error in a depth direction increases. On the other hand, since the contour is no longer arc-shaped but a linear shape at a far distance, the center of the cluster gets closer to the contour, which makes the estimated position also get closer to the true center position.

In the next two subsections, we try to improve the accuracy of the LSM and the MLE by dealing with aforementioned two phenomena; collapse of the contour's shape and the decrease of data points belonging to the contour, in turn.

C. *Reflected beam intensity filter*

In order to improve accuracies of the proposed non-linear LSM and non-linear MLE with known radius at a far distance, we focused on eliminating data points with large noise which cause a collapse of the contour's shape and obtaining arc-shaped contour. Since S/N ratios of such data points are worse than the others, we implemented a reflected beam intensity filter which eliminates data points whose reflected beam intensities are less than α% of the highest intensity in the contour. Estimate errors of the three methods with a reflected beam intensity filter whose filtering threshold was set to be 0%, 40%, and 80%, respectively, are shown in Fig. 10.

From Fig. 10, we can see that by increasing the threshold of the filter, the estimate errors of the CDM tend to decrease and those of the LSM and the MLE tend to increase. With respect to the CDM, since the contour become a linear shape by eliminating data points with large noise arising around the circle's edge, the center of the cluster gets closer to the contour, which makes the estimated position also get closer to the true center position. On the other hands, even though the shape of the contour becomes accurate, estimate errors of the LSM and the MLE become worse. This is considered to be caused by the elimination of valuable data points belonging to the contour.

D. *Improving an angular resolution by a pan unit*

From the previous discussion, it is considered that the accuracy of the LSM and the MLE are strongly dependent on

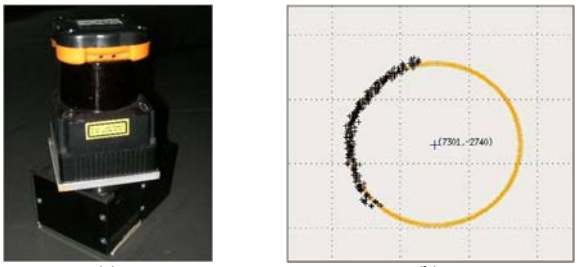

(a) (b)

Fig. 11 (a) A combination of the LRF and the pan unit. (b) Obtained data by using the pan unit.

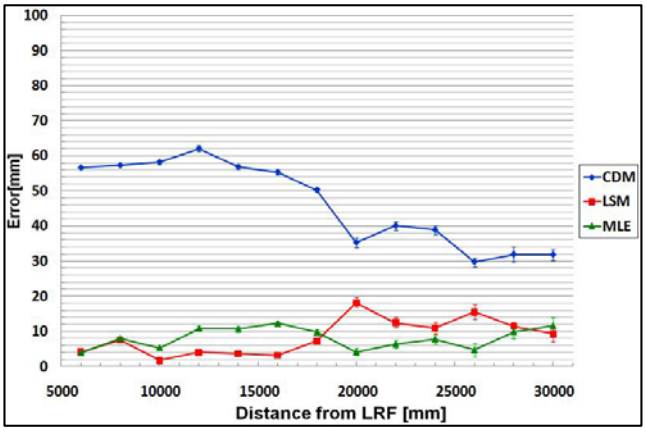

Fig. 12 Estimate errors of the three methods with pan unit. The angular resolution of the LRF was improved about 17 times.

the number of the data points or the length of the contour regardless of the accuracy of the contour's shape. Since we can make the length of the contour longer by using multiple LRFs, here we consider increasing the number of data points belonging to the contour by improving the angular resolution of the LRF using a pan unit.

In order to increase the number of data points, we set the moving head pan unit SPU-01 which can pan by the angular resolution of 0.015 deg from SUSTAINable Robotics beneath the LRF as shown in Fig. 11 (a). Since the angular resolution of the LRF can be improved about 17 times by using the pan unit, by using 17 different scanned results, we can observe a dense contour as shown in Fig. 11 (b). Estimate errors of three methods with the pan unit are shown in Fig. 12.

From Fig. 12, we can say that estimate errors of the LSM and the MLE significantly decrease by improving the angular resolution using the pan unit. Especially, estimate errors of the MLE are stable through all distances and are less than 12 mm. Moreover, we could decrease the variance of the estimate error at each distance compared with Fig. 7, which is necessary for surveys in construction field to determine the measured position precisely.

E. *An application to surveys in construction fields*

We applied the proposed position measurement system to construction fields as shown in Fig. 13. In the system, the LRF is set at a higher position than human height by using the tripod stand and also kept horizontal by using the leveling system. The data acquired from the LRF are sent to the processing computer in which the center positions of the cylindrical reference bars are estimated. Then, the estimated

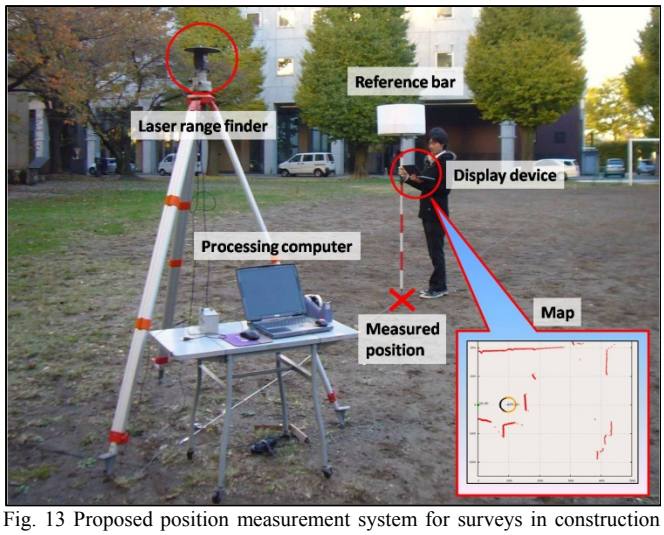

Fig. 13 Proposed position measurement system for surveys in construction fields.

center positions are sent to the mobile display device and the worker can easily gain information on where the current measured position is and where objective positions are in the construction field through a wireless network.

Moreover, the worker can easily construct the proposed position measurement system even based on different OSs because the system is implemented by using RT-Middleware. For this application the system is implemented based on Windows XP for the processing computer and Ubuntu 8.04 for the mobile display device.

IV. CONCLUSION

This paper proposes an accurate long-distance position measurement system for cylindrical objects using LRFs which can be used for surveying tasks in construction fields. This long-distance position measurement system is superior to conventional measurement systems such as a Total Station from the point of view of ease of use, cost-efficiency, and working hour efficiency. However, the most important part of the algorithm is how to estimate the center position of the cylindrical reference bar based on observed data points from the LRF, so we adopted three methods: the CDM, the non-linear LSM with known radius, and the non-linear MLE with known radius. We revealed that the non-linear LSM and the non-linear MLE with known radius (these are the novel approaches to estimate the center position of the circle) gave fewer errors than the CDM. Especially, we achieved the estimate error of the non-linear MLE to be less than 12 mm for a wide range of distances by using the pan unit and improving the angular resolution of the LRF. Also we applied the proposed position measurement system to construction fields.

In our future work, we intend to create a more complete position measurement system where multiple LRFs are available. In principle, circle fitting of both the LSM and the MLE tends to be more accurate when an arc-shaped contour becomes longer, so using multiple LRFs and making the arc-shaped contour longer will give us a more accurate center position of the cylindrical reference bar.

REFERENCES

[1] J. H. Lee and H. Hashimoto, "Intelligent Space - Concept and Contents," *Advanced Robotics*, vol. 16, no. 3, pp. 265-280, 2002.

[2] D. Brscic and H. Hashimoto, "Mobile Robot as Physical Agent of Intelligent Space," *Journal of Computing and Information Technology*, vol. 17, no. 1, pp. 81-94, 2009.

[3] Nikon, *Total Technology: Total Station* [Online]. Available: http://www.nikon.com/about/technology/life/surveying/index.htm

[4] J. E. Guivant, F. R. Masson, and E. M. Nebot, "Simultaneous Localization and Map Building Using Natural Features and Absolute Information," *Robotics and Autonomous Systems*, vol. 40, no. 2-3, pp. 79-90, 2002.

[5] J. Vandorpe, H. V. Brussel, and H. Xu, "Exact Dynamic Map Building for a Mobile Robot using Geometrical Primitives Produced by a 2D Range Finder," in *Proceedings of the IEEE International Conference on Robotics and Automation*, pp. 901-908, 1996.

[6] P. Nunez, R. Vazquez-Martin, A. Bandera, and F. Sandoval, "An Algorithm for Fitting 2-D Data on the Circle: Applications to Mobile Robotics," *IEEE Signal Processing Letters*, vol. 15, pp. 127-130, 2008.

[7] K. Kanatani, "Unified Computation of Strict Maximum Likelihood for Geometric Fitting," in *Proceedings of the IS&T/SPIE 21st Annual Symposium*, EI103: 3D Imaging Metrology, 2009.

[8] K. Kanatani, "Performance Evaluation of Accurate Ellipse Fitting," in *Proceedings of the 21st International Conference on Image and Vision Computing*, pp. 7-12, 2006.

[9] W. Chojnacki, M.J. Brooks, A. van den Hengel, and D. Gawley, "On the Fitting of Surfaces to Data with Covariances," *IEEE Transactions on Pattern Analysis and Machine Intelligence*, vol. 22, no. 11, pp. 1294–1303, 2000.

[10] J. Ryde and H. Hu, "Fast Circular Landmark Detection for Cooperative Localization and Mapping," in *Proceedings of the IEEE International Conference on Robotics and Automation*, pp. 2745-2750, 2005.

[11] N. Chernov and C. Lesort, "Least Square Fitting of Circles," *Journal of Mathematical Imaging and Vision*, vol. 23, pp. 239-251, 2005.

[12] K. Kanatani, "Statistical Optimization for Geometric Fitting: Theoretical Accuracy Analysis and High Order Error Analysis," *International Journal of Computer Vision*, vol. 80, no. 2, pp. 167-188, 2008.

[13] N. Ando, T. Suehiro, K. Kitagaki, T. Kotoku, and W. K. Yoon, "RT-Middleware: Distributed Component Middleware for RT (Robot Technology)," in *Proceedings of the IEEE/RSJ International Conference on Intelligent Robotics and Systems*, pp. 3555-3560, 2005.

[14] Hokuyo Automatic Co., Ltd., *UTM-30LX* [Online]. Available: http://www.hokuyo-aut.jp/02sensor/07scanner/utm_30lx.html

[15] H. Tamura, T. Sasaki, H. Hashimoto, and F. Inoue, "Shape Based Position Measurement Method Using Laser Range Finders," in *Proceedings of the International Conference on Ubiquitous Robotics and Ambient Intelligence*, pp.570-574, 2009.

[16] D. Brscic and H. Hashimoto, "Comparison of Robot Localization Methods Using Distributed and Onboard Laser Range Finders," in *Proceedings of the IEEE/ASME International Conference on Advanced Intelligent Mechatronics*, pp.746-751, 2008.

[17] T. Sasaki and H. Hashimoto, "Design and Implementation of Distributed Sensor Network for Intelligent Space Based on Robot Technology Components," in *Proceedings of the 2nd International Conference on Human System Interaction*, pp.400-405, 2009.